



## 1. INTRODUCTION

In many manufacturing processes such as hot rolling, hot extrusion, wire drawing, crystal growing, continuous casting and fibre drawing, heat transfer occurs between a moving material and the ambient medium. In most of the cases, the moving material is hotter than the surroundings and the heat transfer to the ambient occurs at the surface of the moving material. In the case of wire drawing and continuous casting processes, the material is cooled by passing it through a colder ambient medium like water or, in some cases, just quiescent ambient air. In the design of nuclear reactor fuel elements it is necessary to consider their temperature behaviour during various types of power transients. Under some conditions, for example, during a coolant pump failure, the heat removal to the cooling fluid may be solely by free convection. To obtain some insight into the convective process it is necessary to consider how the free-convection boundary layer is influenced when the heated surface is undergoing a thermal transient.

Stokes [1] first presented an exact solution to the Navier–Stokes equation which is for the flow of a viscous incompressible fluid past an impulsively started infinite horizontal plate in its own plane. Such a flow past an impulsively started semi-infinite horizontal plate was first presented by Stewartson [2]. However, such an analysis has not been carried out in case of the flow past an impulsively started semi-infinite isothermal vertical plate. Following Stokes [1] analysis, Soundalgekar [3] was the first to present an exact solution to the flow of a viscous fluid past an impulsively started infinite vertical plate in its own plane. The solution was derived by the usual Laplace-transform technique and the effects of heating or cooling of the plate on the flow-field were discussed through Grashof number. Soundalgekar and Patil [4, 5] have studied Stoke’s problem for infinite vertical plate with uniform heat flux and variable temperature. Soundalgekar [6] analysed the mass transfer effects on the flow past an impulsively started infinite isothermal vertical plate. Again, Soundalgekar et al. [7] have considered the flow past an impulsively started infinite vertical plate with uniform heat flux and mass transfer. Das et al. [8] have studied the flow past an impulsively started infinite isothermal vertical plate with constant mass flux. In all above studies [4–8], the dimensionless governing equations are solved by using Laplace-transform technique.

Hall [9] solved the flow past an impulsively started semi-infinite horizontal plate using numerical technique. He employed a finite-difference method of a mixed

explicit–implicit type, which is free from any restrictions on the mesh-size and, hence, it is a convergent and stable finite-difference technique. Velocity profiles were computed for different values of the nondimensional time  $T$ . Also the variation of the surface shear with respect to time  $T$  was shown graphically. Muthukumaraswamy and Ganesan [10] obtained the finite-difference solution of the flow past an impulsively started semi-infinite vertical plate with heat and mass transfer. Here the plate temperature and the concentration level near the plate are considered to be uniform. Again, Muthukumaraswamy and Ganesan [11] have analysed the mass transfer effects on flow past an impulsively started vertical plate with variable surface temperature and mass flux using finite-difference technique. Pure heat transfer effects were not taken into consideration in [10, 11].

However, the heat transfer effects alone play an important role in some industrial applications like food processing, steel and ceramic industries. An example is the study of cracking behaviour in ceramic industries. Cracking due to improper drying is a major loss to the ceramic industry. The removal of moisture in ceramic product is very important. The temperature isotherms for various shapes, sizes and materials for various rates of temperature rise in furnaces. This will help in understanding the cracking behaviour. Hence, we have studied the flow past an impulsively started semi-infinite isothermal vertical plate using implicit finite-difference scheme of Crank–Nicolson type. The transient and steady-state velocity and temperature profiles are shown graphically. The effect of local as well as average skin friction and Nusselt number are studied. As a check, we have computed the numerical values of the velocity and temperature profiles from the exact solution derived by Soundalgekar [3] for  $t = 0.2$ ,  $Gr = 5, 10$  and  $Pr = 0.71$  and also from the present analysis, and these are found to agree in an excellent way.

## 2. MATHEMATICAL ANALYSIS

Consider a semi-infinite vertical plate held stationary in an infinite mass of viscous incompressible fluid, both being maintained at constant temperature  $T'_\infty$  initially. The physical model of the problem is given in *figure 1*. Here the  $x$ -axis is taken along the plate in the vertically upward direction and the  $y$ -axis is chosen normal to the plate. At time  $t' > 0$ , the plate is given an impulsive motion in the vertical direction in its own plane so that it starts moving with a constant velocity  $u_0$  and the plate temperature is raised to  $T'_w$  causing the existence of

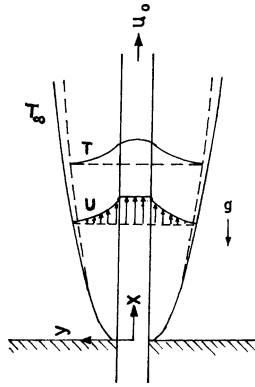


Figure 1. Physical model of the problem.

temperature difference near the plate. This in turn creates buoyancy forces, and hence, we can assume Boussinesq's approximation. Then under these physical conditions, the laminar flow can be shown to be governed by the following system of equations:

$$\frac{\partial u}{\partial x} + \frac{\partial v}{\partial y} = 0 \tag{1}$$

$$\frac{\partial u}{\partial t'} + u \frac{\partial u}{\partial x} + v \frac{\partial u}{\partial y} = g\beta(T' - T'_\infty) + \nu \frac{\partial^2 u}{\partial y^2} \tag{2}$$

$$\frac{\partial T'}{\partial t'} + u \frac{\partial T'}{\partial x} + v \frac{\partial T'}{\partial y} = \alpha \frac{\partial^2 T'}{\partial y^2} \tag{3}$$

with the following initial and boundary conditions:

$$t' \leq 0: \quad u = 0, \quad v = 0, \quad T' = T'_\infty$$

$$t' > 0:$$

$$u = u_0, \quad v = 0, \quad T' = T'_w \quad \text{at } y = 0 \tag{4}$$

$$u = 0, \quad T' = T'_\infty \quad \text{at } x = 0$$

$$u \rightarrow 0, \quad T' \rightarrow T'_\infty \quad \text{as } y \rightarrow \infty$$

We now introduce the following nondimensional quantities:

$$\begin{aligned} X &= \frac{xu_0}{\nu}, & Y &= \frac{yu_0}{\nu}, & U &= \frac{u}{u_0} \\ V &= \frac{v}{u_0}, & t &= \frac{t'u_0^2}{\nu} \\ Gr &= \frac{\nu g\beta(T'_w - T'_\infty)}{u_0^3} \\ T &= \frac{T' - T'_\infty}{T'_w - T'_\infty}, & Pr &= \frac{\nu}{\alpha} \end{aligned} \tag{5}$$

in equations (1)–(4) which leads to

$$\frac{\partial U}{\partial X} + \frac{\partial V}{\partial Y} = 0 \tag{6}$$

$$\frac{\partial U}{\partial t} + U \frac{\partial U}{\partial X} + V \frac{\partial U}{\partial Y} = GrT + \frac{\partial^2 U}{\partial Y^2} \tag{7}$$

$$\frac{\partial T}{\partial t} + U \frac{\partial T}{\partial X} + V \frac{\partial T}{\partial Y} = \frac{1}{Pr} \frac{\partial^2 T}{\partial Y^2} \tag{8}$$

and the initial and boundary conditions are

$$t \leq 0: \quad U = 0, \quad V = 0, \quad T = 0$$

$$t > 0:$$

$$U = 1, \quad V = 0, \quad T = 1 \quad \text{at } Y = 0 \tag{9}$$

$$U = 0, \quad T = 0 \quad \text{at } X = 0$$

$$U \rightarrow 0, \quad T \rightarrow 0 \quad \text{as } Y \rightarrow \infty$$

An implicit finite-difference scheme of Crank–Nicolson type has been employed to solve the nonlinear coupled equations (6)–(8) with the conditions (9). The dimensionless governing equations are reduced to tridiagonal system of equations. Such a system of equations is solved by using Thomas algorithm as described in Carnahan et al. [12]. The region of integration is considered as a rectangle with sides  $X_{\max}(= 1)$  and  $Y_{\max}(= 14)$ , where  $Y_{\max}$  corresponds to  $Y = \infty$ , which lies very well outside the momentum, energy and concentration boundary layers. The maximum of  $Y$  was chosen as 14 after some preliminary investigations so that the last two of the boundary conditions (11) are satisfied within the tolerance limit  $10^{-5}$ . We take the mesh sizes in the  $X$  and  $Y$  directions, during computation, as  $\Delta X = 0.05$  and  $\Delta Y = 0.25$  and the time step level at  $\Delta t = 0.01$ . The stability of the finite-difference scheme and numerical technique used in this problem is discussed in Muthukumaraswamy and Ganesan [10].

### 3. DISCUSSION OF RESULTS

Representative numerical results for the uniform wall temperature will be discussed in this section. In order to ascertain the accuracy of our numerical results we have compared our present results with the exact solutions of those of Soundalgekar [3] for both the velocity and the temperature for  $Gr = 5, 10, t = 0.2, Pr = 0.71$  (here  $\eta = Y/\sqrt{2t}$ ) and these are shown in figures 2 and 3. The velocity profiles are shown in figure 2 and we observe that the agreement with the exact solution of  $U$  is excellent. Likewise in figure 3 for the temperature profiles given by  $T = \text{erfc}(\eta\sqrt{Pr})$  (Soundalgekar [3]) we find that the agreement is also excellent.

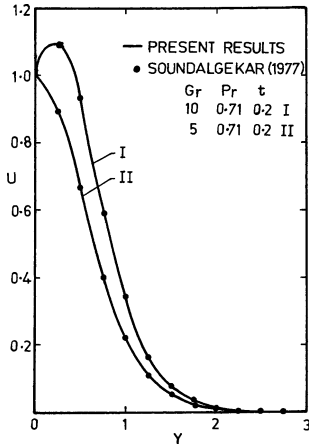


Figure 2. Comparison of velocity profiles.

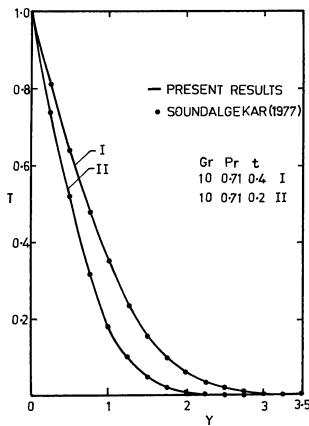


Figure 3. Comparison of temperature profiles.

The transient and steady-state velocity profiles for different thermal Grashof number and Prandtl number ( $Pr = 0.71$  (air),  $7.0$  (water)) are shown in figure 4. In the initial stage, at small values of time  $t$ , the transient velocity of air is observed to increase rapidly, attaining maximum value at  $t = 0.2$  at small values of the Grashof number as compared to large values of the Grashof number. Hence, we conclude that the maximum value of the transient velocity at small values of time  $t$  decreases as the Grashof number increases. Then as time  $t$  increases, the maximum value of the transient velocity is found to decrease. The velocity boundary layer is seen to grow in the direction of motion of the plate. It is observed that near the leading edge of a semi-infinite vertical plate moving in a fluid, where in the boundary layer develops along the direction of the plate. However, the time required for the velocity to reach the steady state depends upon both the Prandtl number and the Grashof number.

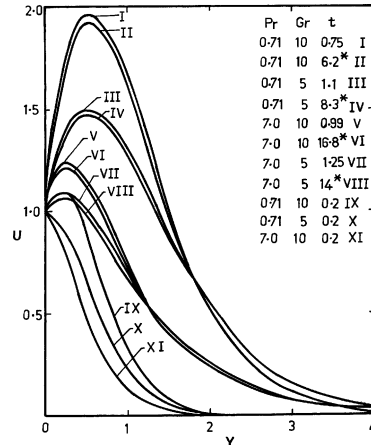


Figure 4. Transient velocity profiles at  $X = 1.0$  (\*, steady state).

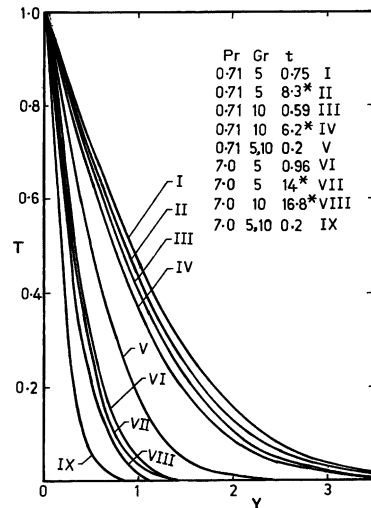


Figure 5. Transient temperature profiles at  $X = 1.0$  (\*, steady state).

For  $Pr < 1$ , the time required for the velocity to reach its steady state decreases as the Grashof number increases but for  $Pr > 1$ , it is just the opposite, namely, the time required to reach its steady state increases as the Grashof number  $Gr$  increases. Moreover, the steady-state velocity increases as the Grashof number  $Gr$  increases for  $Pr > 1$ , but the steady-state velocity decreases with increasing the Grashof number for  $Pr < 1$ . In general, the transient or the steady-state velocity for  $Pr > 1$  is always less than that for  $Pr < 1$ .

The transient and steady-state temperature profiles are shown in figure 5 which are quite interesting. At small values of time  $t$  the transient temperature is not affected by the variation in Grashof number for both  $Pr \geq 1$ .

No buoyancy effect is seen at the beginning because the fluid is not hot enough to introduce significant buoyancy force. As time elapses, thermal buoyancy effects are seen easily. It is interesting to note that the temperature maxima do not occur at steady state but during the transient process. It is known that Prandtl number plays an important role in flow phenomena because it is a measure of the relative magnitude of viscous fluid boundary layer thickness to the thermal boundary layer thickness. It is observed that the thermal boundary layer is found to be thicker in air than in water, as seen in *figure 5* and as expected for the lower Prandtl number. This shows that the buoyancy effect on the temperature distribution is very significant in air. However, the behaviour of the transient temperature to reach its steady state is similar to that of the transient velocity.

Knowing the velocity and the temperature field, it is customary to study the skin friction and the rate of heat transfer both in their transient and steady-state conditions. The local as well as average skin friction and Nusselt number are given by

$$\tau_x = -\left(\frac{\partial U}{\partial Y}\right)_{Y=0} \quad (10)$$

$$\bar{\tau} = -\int_0^1 \left(\frac{\partial U}{\partial Y}\right)_{Y=0} dX \quad (11)$$

$$Nu_x = -X \left(\frac{\partial T}{\partial Y}\right)_{Y=0} \quad (12)$$

$$\bar{Nu} = -\int_0^1 \left(\frac{\partial T}{\partial Y}\right)_{Y=0} dX \quad (13)$$

The derivatives involved in equations (10)–(13) are evaluated by using a five-point approximation formula and then the integrals are evaluated by using Newton–Cotes closed integration formula.

The local skin friction values were evaluated from equation (10) and plotted in *figure 6* as a function of the axial coordinate  $X$ . The local wall shear stress decreases as  $X$  increases. It is observed that the local skin friction increases with increasing the Prandtl number but decreases with increasing the Grashof number  $Gr$ . The value of the skin friction becomes negative which shows that after some time there occurs a reverse type of flow near the moving plate. Physically this is also true as the motion of the fluid is due to plate moving in the vertical direction against the gravitational field.

The average skin friction is shown in *figure 7* and the influence of the Prandtl and the Grashof number is the same as in case of the local skin friction. It decreases

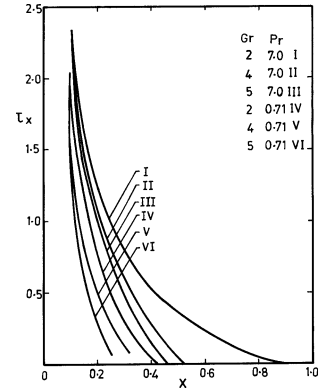


Figure 6. Local skin friction.

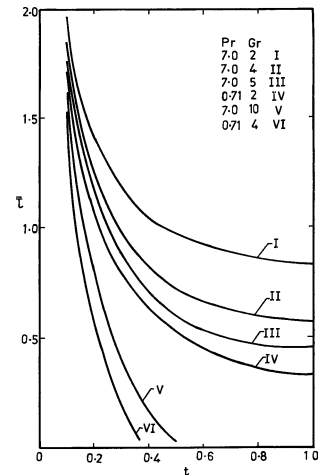


Figure 7. Average skin friction.

with an increase in time for small values of  $t$  but in case of water ( $Pr = 7.0$ ), at large values of time  $t$ , the average skin friction is almost unaffected by time for all values of the Grashof number. However, for  $Pr < 1$ , the average skin friction is found to be affected only at very small values of time  $t$  when the Grashof number is high.

The local and the average Nusselt number are shown in *figures 8* and *9*, respectively. We observe from *figure 8* that the local Nusselt number increases with increasing the Prandtl number and the Grashof number. The average Nusselt number for different thermal Grashof number is shown in *figure 9*. The rate of heat transfer for air is found to decrease with increasing time  $t$  at small values of time  $t$ , but at large time  $t > 0.5$ , it is not significantly affected by time. However, an increase in the Grashof number leads to an increase in the rate of heat transfer.

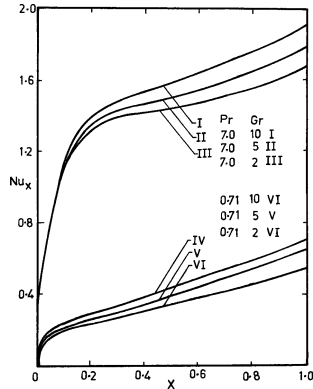


Figure 8. Local Nusselt number.

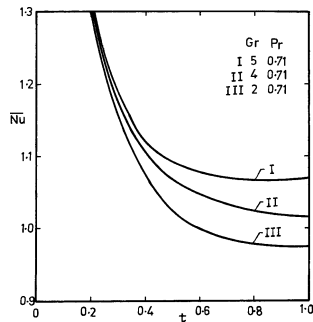


Figure 9. Average Nusselt number.

#### 4. CONCLUSIONS

1. When the Grashof number increases less time is required to reach the steady state velocity or temperature value when  $Pr < 1$  as compared to that for  $Pr > 1$ .
2. The transient or the steady-state velocity for  $Pr > 1$  is always less than that for  $Pr < 1$ .
3. At small values of time  $t$ , the transient temperature is not affected due to variation in the value of the Grashof number, for both  $Pr \geq 1$ .
4. The local or the average skin friction increases with increasing the Prandtl number but decreases with increasing the Grashof number.
5. The local skin friction decreases with an increase in time at small values of time  $t$ . But for water,  $Pr = 7.0$ , the average skin friction is almost unaffected by time

for all values of the Grashof number. However, for  $Pr < 1$ , and at high values of the Grashof number, the average skin friction is affected only at small values of time  $t$ .

6. The local Nusselt number increases with increasing both the Prandtl and the Grashof number.
7. The average Nusselt number increases with increasing the Grashof number.

#### REFERENCES

- [1] Stokes G.G., On the effect of internal friction of fluids on the motion of pendulums, *Cambr. Phil. Soc.* 9 (1851) 8-126.
- [2] Stewartson K., On the impulsive motion of a flat plate in a viscous fluid, *Quart. J. Mech. Appl. Math.* 4 (1951) 182-198.
- [3] Soundalgekar V.M., Free convection effects on the Stokes problem for an infinite vertical plate, *Trans. ASME J. Heat Tran.* 99 (1977) 499-501.
- [4] Soundalgekar V.M., Effects of mass transfer and free convection currents on the flow past an impulsively started vertical plate, *ASME J. Appl. Mech.* 46 (1979) 757-760.
- [5] Soundalgekar V.M., Patil M.R., Stokes problem for a vertical infinite plate with variable temperature, *Astrophysics and Space Science* 59 (1978) 503-506.
- [6] Soundalgekar V.M., Patil M.R., Stokes problem for a vertical plate with constant heat flux, *Astrophysics and Space Science* 70 (1980) 179-182.
- [7] Soundalgekar V.M., Birajdar N.S., Darwekar V.K., Mass transfer effects on the flow past an impulsively started infinite vertical plate with variable temperature or constant heat flux, *Astrophysics and Space Science* 100 (1984) 159-164.
- [8] Das U.N., Ray S.N., Soundalgekar V.M., Mass transfer effects on flow past an impulsively started infinite vertical plate with constant mass flux — an exact solution, *Heat Mass Tran.* 31 (1996) 163-167.
- [9] Hall M.G., Boundary layer over an impulsively started flat plate, *Proc. Roy. Soc. London Ser. A* 310 (1969) 401-414.
- [10] Muthukumaraswamy R., Ganesan P., Unsteady flow past an impulsively started vertical plate with heat and mass transfer, *Heat Mass Tran.* 34 (1998) 187-193.
- [11] Muthukumaraswamy R., Ganesan P., Flow past an impulsively started vertical plate with variable surface temperature and mass flux, *Heat Mass Tran.* 34 (1999) 487-493.
- [12] Carnahan B., Luther H.A., Wilkes J.O., *Applied Numerical Methods*, Wiley, New York, 1969.